Clays and Clay Minerals, Vol. 57, No. 4, 452–464, 2009.

THE EFFECT OF STRUCTURAL ORDER ON NANOTUBES DERIVED FROM KAOLIN-GROUP MINERALS

JAKUB MATUSIK[1,*], ADAM GAWEŁ[1], ELŻBIETA BIELAŃSKA[2], WŁADYSŁAW OSUCH[3], AND KRZYSZTOF BAHRANOWSKI[1]

[1] AGH University of Science and Technology, Faculty of Geology, Geophysics and Environmental Protection, al. Mickiewicza 30, 30-059 Krakow, Poland
[2] Institute of Catalysis and Surface Chemistry, Polish Academy of Sciences, ul. Niezapominajek 8, 30-239 Krakow, Poland
[3] AGH University of Science and Technology, Faculty of Metal Engineering and Industrial Computer Science, al. Mickiewicza 30, 30-059 Krakow, Poland

Abstract—Kaolin-group clay minerals can be modified to form nanotubular and mesoporous structures with interesting catalytic properties, but knowledge of the best methods for preparing these structures is still incomplete. The objective of this study was to investigate intercalation/deintercalation as a method for the delamination and rolling of kaolinite layers in relation to structural order. To prepare nanotubular material, kaolinites of different crystallinities and halloysite (all from Polish deposits) were chosen. The experimental procedure consisted of four stages: (1) preparation of a dimethyl sulfoxide precursor intercalate; (2) interlayer grafting with 1,3-butanediol; (3) hexylamine intercalation; and (4) deintercalation of amine-intercalated minerals using toluene as the solvent. Structural perturbations and changes in the morphology of the minerals were examined by X-ray diffraction, Fourier transform infrared spectroscopy, differential scanning calorimetry, and transmission electron microscopy (TEM). The number of rolled kaolinite layers depended heavily on the efficiency of the intercalation steps. An increase in the structural disorder and extensive delamination of the minerals subjected to chemical treatment were recorded. Kaolinite particles which exhibited tubular morphology or showed rolling effects were observed using TEM. The nanotubes formed were ~30 nm in diameter, with their length depending on the particle sizes of the minerals.

Key Words—Halloysite, Intercalation, Kaolinite, Nanotubes, Rolling, Structural Order.

INTRODUCTION

Chemical modifications of clay minerals have great potential in scientific and industrial applications (Murray, 2000; Serwicka and Bahranowski, 2004). The ability to combine the properties of an inorganic matrix with organic molecules at a molecular level allows for the design of improved nanocomposite materials (Tunney and Detellier, 1997; Gardolinski and Lagaly, 2005a; Elbokl and Detellier, 2006; Liu *et al.*, 2008). Nanotubular and mesoporous materials have received much attention because of their interesting catalytic properties (Zimowska *et al.*, 2007). Examples of such solids include derivatives structurally related to the FSM-16 (Folded Sheet Material) and MCM-41 (Mobile Crystalline Material) compounds (Inagaki *et al.*, 1993; Lin and Mou, 1996). FSM-16 was obtained from the layered mineral, kanemite, and is constructed from folded siliceous sheets which form mesopores. MCM-41 consists of hexagonal arrays of nm-sized cylindrical pores and can be synthesized by condensation of silica onto cylindrical cationic micelles. Fibrous and tubular structures, of natural or synthetic origin, are versatile, relatively cheap, and have large surface areas (Nakagaki and Wypych, 2007). The chemical composition and surface reactivity of such materials can be controlled easily by increasing the concentration of active sites or by the immobilization of active molecules (Nakagaki *et al.*, 2006; Machado *et al.*, 2008).

Kaolinite, $Al_2Si_2O_5(OH)_4$, is a dioctahedral 1:1 phyllosilicate, used in the synthesis of nanotubes and mesoporous silica (Dong *et al.*, 2003; Madhusoodana *et al.*, 2006). Dong *et al.* (2003) carried out experiments which involved surfactant intercalation, acid addition, and hydrothermal treatment. The formation of nanotubes was related to significant perturbations and/or destruction of the initial layered structure.

Many factors, such as Fe content, crystallinity, surface tension, strength of interlayer bonding, and environment and history of formation, were reported to influence the observed morphology of kaolin-group minerals (Hope and Kittrick, 1964; Joussein *et al.*, 2005). Tubular morphology was related to dimensional misfit between the tetrahedral and octahedral sheets (Bates *et al.*, 1950). A more recent study (Singh, 1996) revealed that when interlayer hydrogen bonds of kaolinite are weakened, layers tend to roll in order to correct the misfit between sheets. In the case of strong hydrogen bonds, tetrahedral rotation occurs and planar particles are observed.

* E-mail address of corresponding author:
jakub_matusik@wp.pl
DOI: 10.1346/CCMN.2009.0570406

Nitrobenzene treatment leads to the breaking of kaolinite interlayer bonding and causes crystallites to curl (Hope and Kittrick, 1964). Singh and Mackinnon (1996) reported that planar kaolinite particles may be transformed into tubular halloysite by repeated intercalation with potassium acetate. Such treatment produced a highly disordered mineral, as recorded by Wiewióra and Brindley (1969). The formation of a partially delaminated structure with halloysite-like morphology was also observed in the reactions with ammonium acetate and octylamine (Weiss and Russow, 1963; Poyato-Ferrera *et al.*, 1977). However, an effective method which successfully delaminates kaolinite layers forming halloysite-like tubes, without Si/Al framework dissolution, was described by Gardolinski and Lagaly (2005b). In their work, intercalation of kaolinite using long-chain amines was performed in order to weaken the hydrogen bonds.

In the present study, kaolin-group minerals from well known Polish deposits were treated according to the intercalation/deintercalation method proposed by Gardolinski and Lagaly (2005b). The main objective was to investigate the delamination and rolling of kaolinite layers in relation to structural order. Secondly, the reactivity of these clays towards the intercalation and grafting processes was examined. Changes in the thicknesses of the kaolin particles during the experimental stages were also studied.

MATERIALS AND METHODS

Materials

Halloysite and kaolinites with different degrees of structural order were used and are labeled as follows: 'Maria III' (well crystallized kaolinite) – M; 'Jaroszów' (poorly crystallized kaolinite) – J; and 'Dunino' (halloysite and kaolinite mixture) – H. The <2 μm fraction, separated by centrifugation, was used for all reactions. In addition, a <40 μm fraction of the 'Maria III' deposit was used (labeled M40). Deionized water and analytical, reagent-grade chemicals were used throughout. Dimethyl sulfoxide (DMSO), ethanol, acetone, diethyl ether, cyclohexane, and toluene (T) were obtained from POCH-Polish Chemical Reagents. Hexylamine (HX) and 1,3-butanediol (B) were purchased from Merck and Fluka, respectively.

Experimental procedure

Synthesis followed the procedure proposed by Gardolinski and Lagaly (2005a, 2005b), consisting of four experimental stages performed for all samples. Intercalates of minerals with dimethyl sulfoxide were prepared according to the method described by Olejnik *et al.* (1968). The precursors obtained were reacted with 1,3-butanediol in order to synthesize grafted derivatives. The conditions for the synthesis and post-synthesis washing have been described elsewhere (Murakami *et al.*, 2004; Gardolinski and Lagaly, 2005a). Afterwards, the grafted compounds were subjected to intercalation reactions with hexylamine (Gardolinski and Lagaly, 2005b). In the next stage, amine molecules were deintercalated in experimental conditions identical to those proposed by Gardolinski and Lagaly (2005b). The deintercalation procedure needed a highly non-polar solvent to remove the long-chain amine quickly, thereby promoting separation of the kaolinite layers. Several solvents: toluene, n-hexane, petroleum ether, and carbon tetrachloride, were tested by Gardolinski (J.E.F.C. Gardolinski, pers. comm., 2008). Toluene gave the best results and so was used for the experiments. The products obtained after each experimental step were dried at 60ºC for 24 h.

Analytical methods

Powder X-ray diffraction (XRD) patterns of unoriented samples were recorded, in the range 2–30º2θ in steps of 0.05º2θ, using a Philips APD PW 3020 X'Pert instrument with CuKα radiation and a graphite monochromator. The degree of intercalation was estimated according to the formula: $I_c/(I_c+I_7)$*100%, where I_c was the basal peak intensity of the new intercalate and I_7 was the intensity of the kaolinite 001 peak after intercalation (Churchman *et al.*, 1984). This method provided values for the degree of intercalation, on the basis of diffraction peaks of the intercalated phase (I_c) and the unreacted phase (I_7). In addition, the degree of intercalation was estimated on the basis of kaolinite 001 peak intensity before (I_{7R}) and after (I_7) intercalation, according to the formula: 100%-(I_7/I_{7R})*100%. Decomposition of diffraction peaks in the 20–23º2θ region, necessary for the Aparicio-Galán-Ferrell index calculations (Aparicio *et al.*, 2006), was performed using *WinFit* 1.2.1 software created by Stefan Krumm. The average number of layers per crystallite was calculated from the 002 reflection broadening, using the Scherrer formula (Patterson, 1939). The Fourier transform infrared (FTIR) spectra were collected after 256 scans at 2 cm^{-1} resolution in the region of 4000–400 cm^{-1}using a Bio-Rad FTS-60 spectrometer. Samples were prepared using the standard KBr pellet method (0.5 mg of sample per 200 mg of KBr). Differential calorimetric (DSC) and thermogravimetric (TG) analyses were carried out using a Netzsch STA 409 PC/PG instrument (sample mass: 10 mg, heating rate: 10ºC/min, air flow: 30 mL/min). Observations of the morphology of the samples prepared were collected using a JEOL JSM 7500F field emission scanning electron microscope coupled with TEM mode and a JEOL JEM 200CX transmission electron microscope.

RESULTS AND DISCUSSION

Characterization of raw samples

The XRD patterns of the raw kaolin-group minerals used for the experiments (Figure 1) revealed that both the 'Maria III' (M, M40) and 'Jaroszów' (J) kaolinites

https://doi.org/10.1346/CCMN.2009.0570406 Published online by Cambridge University Press

contained small admixtures of quartz. In addition, the presence of a 10 Å peak indicated that both the M and M40 samples contained small amounts of illite. The presence of illite and mixed-layered smectite-illite was recorded for the J sample. The proportion of halloysite to kaolinite for the dehydrated 'Dunino' sample (H) was estimated using the formamide method proposed by Churchman *et al.* (1984). The tests performed indicated that the ratio of halloysite-(7 Å) to kaolinite was 59:41.

The Hinckley index (k_H), Stoch factor (f_S), and Aparicio-Galán-Ferrell index (AGFI) were taken as a measure of structural order (Hinckley, 1962; Stoch, 1974; Aparicio *et al.*, 2006; Brigatti *et al.*, 2006). For the M and M40 samples, the k_H and f_S values were identical and equal to 1.31 and 0.71, respectively (Bahranowski *et al.*, 1993). For the J and H samples, k_H was calculated as 0.22 and 0.33, while the f_S values were 1.74 and 1.15, respectively (Bahranowski *et al.*, 1993). The AGFI value, which is based on XRD-profile fitting, proved to be less sensitive to admixtures of other minerals than k_H and f_S (Aparicio *et al.*, 2006). The AGFI values calculated for the M, M40, J, and H samples were 1.39, 1.38, 0.37, and 0.63, respectively.

All three crystallinity indexes, as well as the presence of four clearly resolved absorption bands in the OH-stretching region (3700−3600 cm^{-1}) of the IR spectra (Figure 2), confirmed that 'Maria III' is a low-defect kaolinite (Farmer and Russell, 1967; Farmer, 1974). The values of the crystallinity indexes and the changes in the relative intensities and shapes of bands in the OH region (Figure 2) in comparison with the IR spectra of 'Maria III' kaolinite indicated that 'Jaroszów' is a poorly crystallized, high-defect kaolinite (Farmer and Russell, 1967; Farmer, 1974). The very low-intensity absorption band at ~3650 cm^{-1}, for the H sample (Figure 2), is probably related to the presence of water molecules occupying the interlayer space of halloysite (Stoch, 1974).

The structural order of the kaolinites examined is strongly related to the shape of their particles. Well developed hexagonal plates were observed frequently in the M and M40 samples (Figure 3a,b) while rounded particles with edges which were less sharp were characteristic for sample J (Figure 3c). Halloysite observed in the H sample consisted of laths, tubes, and plates (Figure 3d).

Preparation of DMSO derivatives

Intercalation with DMSO was successful for all minerals. In all cases a basal peak of a new derivative of 11.26 Å was observed (Figure 1), in good agreement with values from the literature (Olejnik *et al.*, 1968; Thompson and Cuff, 1985; Hayashi, 1997). The relative increase in peak intensity and/or the appearance of new reflections in the region from 20 to 23º2θ suggested that the DMSO molecules have a tendency to adopt an ordered arrangement and probably induced new order in stacking of layers in the mineral structure (Figure 1). The presence of distinct second- (5.62 Å) and third- (3.73 Å) order reflections for the DMSO intercalates, indicated a high degree of stacking order along the *c* axis (Figure 1).

Regardless of the starting material, the IR spectra of the DMSO intercalates (Figure 2) showed significant changes in the OH-stretching region (3700−3600 cm^{-1}). This involved a simultaneous decrease in the intensity of the 3697 cm^{-1} band, an increase in intensity of the band at ~3663 cm^{-1}, and the appearance of bands at ~3540 cm^{-1}, 3502 cm^{-1}, and 957 cm^{-1}. New sharp bands resulted from the formation of hydrogen bonds between DMSO and mineral interlayer hydroxyls (Olejnik *et al.*, 1968). The kaolinite lattice vibrations (1200−1000 cm^{-1}) also showed perturbations after intercalation. The two most intense bands at ~1033 cm^{-1} and 1008 cm^{-1} were shifted to greater frequencies in the case of the MDS and M40DS samples. In turn, for the JDS and HDS samples, the first band remained unaffected, while the latter was shifted to a greater frequency. These bands were previously assigned to the in-plane Si-O-Si stretching vibrations of kaolinite (Farmer, 1974). The perpendicular Si-O vibrations, observed for all samples in the region 1099−1109 cm^{-1} (Farmer, 1974), were only slightly altered. In addition, a new band was recorded at ~1125 cm^{-1}, for the M40DS sample. Moreover, Si-O-Si bending vibrations found at ~538 cm^{-1} (Farmer, 1974) were shifted to 552 cm^{-1} for the MDS sample, to 550 cm^{-1} for the M40DS sample, and to 545 cm^{-1} for the HDS sample, while it remained unchanged in the case of the JDS sample. A decrease in the intensity of this band was observed in all cases. Much greater shifts of the bands were observed for the MDS and M40DS samples than for the JDS and HDS samples, indicating that after DMSO intercalation the well ordered kaolinites underwent structural perturbations to a greater extent than the poorly ordered samples.

Intercalation was most efficient for the 'Maria III' kaolinite. Regardless of the particle size (<2 μm and <40 μm), the degree of intercalation reached ~95% (MDS, M40DS). The value was less for the 'Jaroszów' kaolinite (JDS) and for the 'Dunino' halloysite (HDS), where it was 85% and 90%, respectively. The degree of intercalation, calculated only on the basis of the kaolin-

Figure 1 (*facing page*). XRD patterns of: (a) M – 'Maria III' kaolinite (<2 μm); (b) M40 – 'Maria III' kaolinite (<40 μm); (c) J – 'Jaroszów' kaolinite (<2 μm); and (d) H – 'Dunino' halloysite (<2 μm) after: DS – DMSO intercalation; B – 1,3-butanediol grafting; HX – hexylamine intercalation; and T – deintercalation by toluene. Abbreviations: Q – quartz, I – illite, S-I – mixed-layered smectite-illite.

https://doi.org/10.1346/CCMN.2009.0570406 Published online by Cambridge University Press

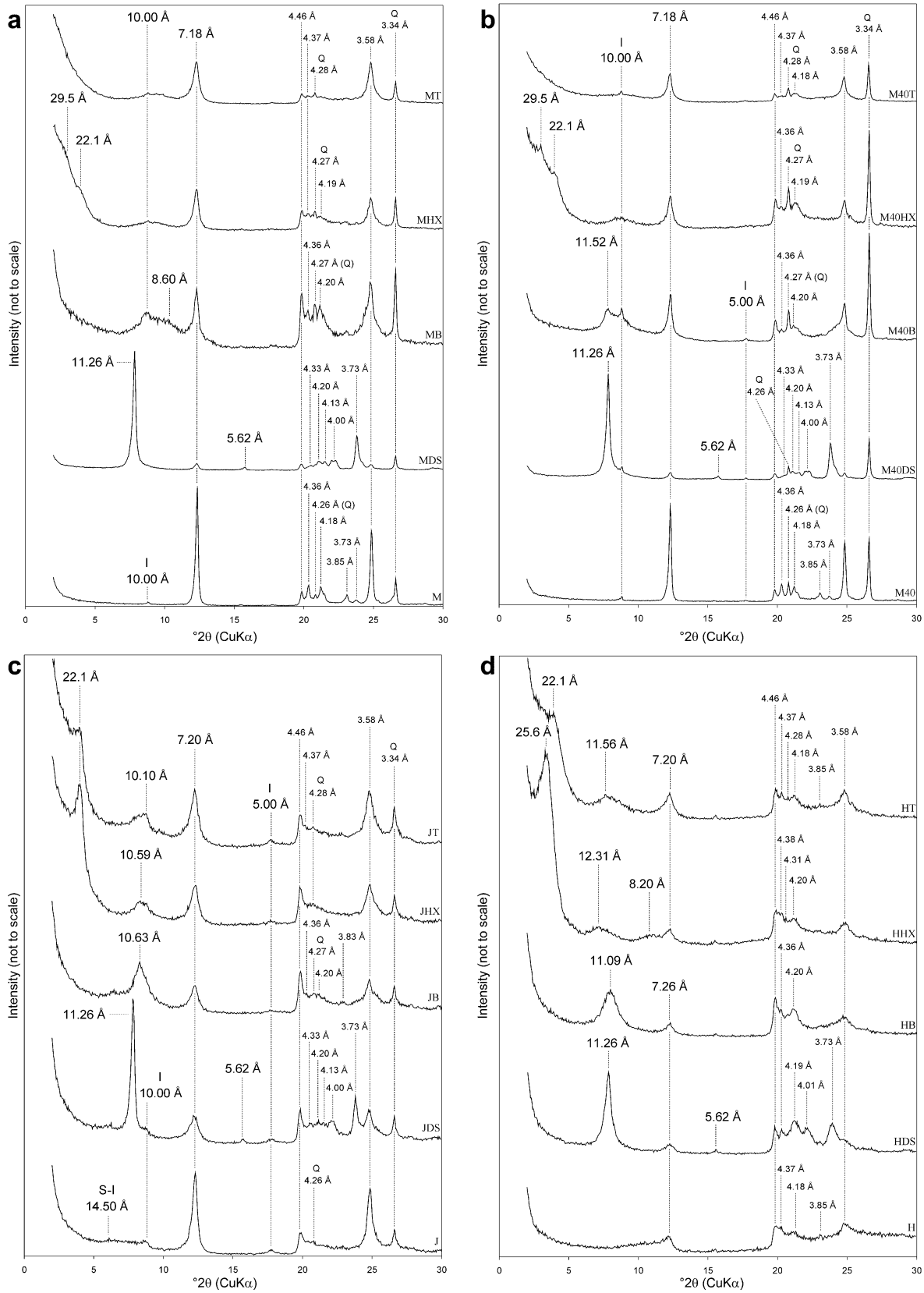

https://doi.org/10.1346/CCMN.2009.0570406 Published online by Cambridge University Press

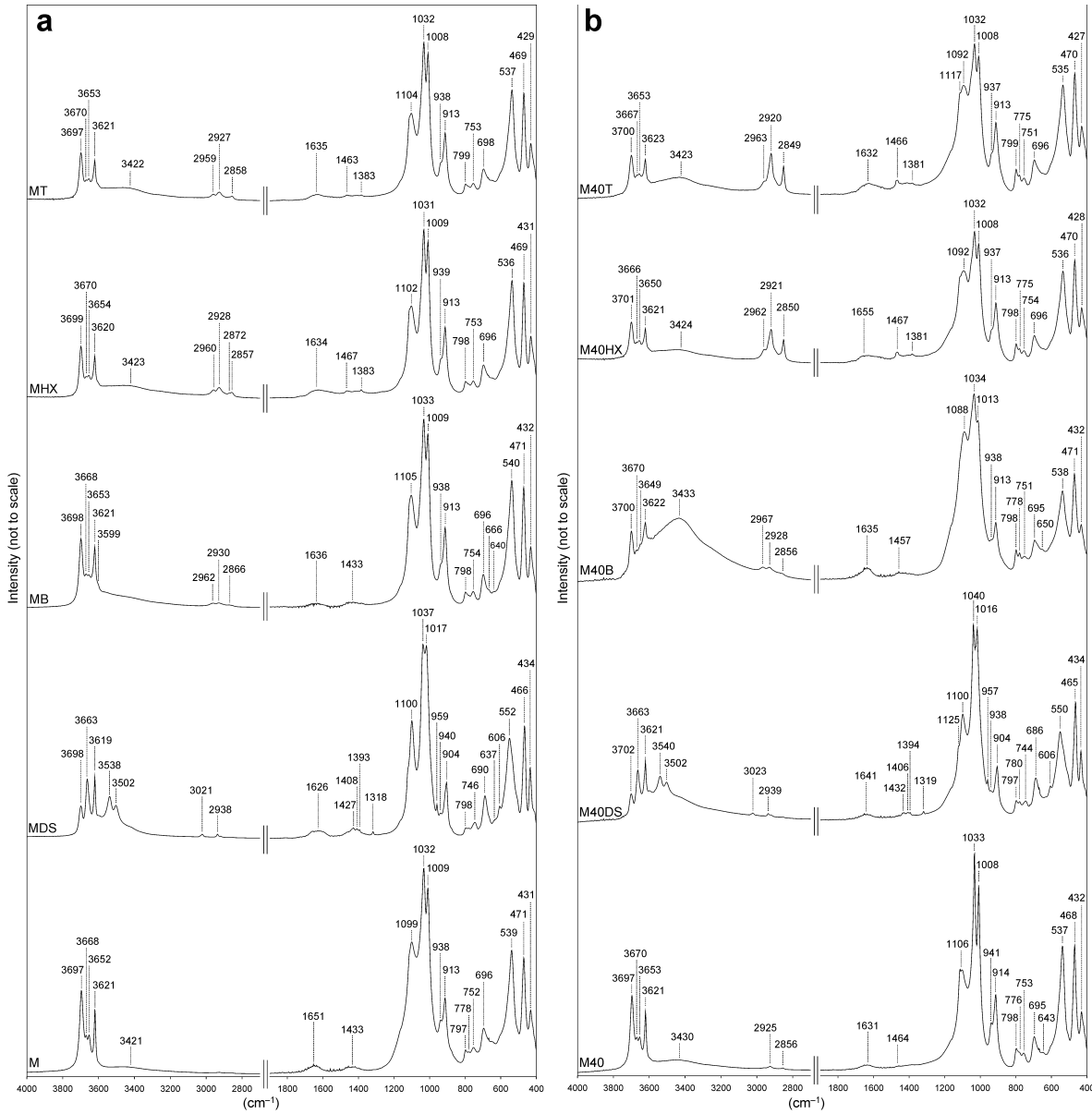

Figure 2 (*above and facing page*). FTIR spectra of: (a) M – 'Maria III' kaolinite (<2 μm); (b) M40 – 'Maria III' kaolinite (<40 μm); (c) J – 'Jaroszów' kaolinite (<2 μm); and (d) H – 'Dunino' halloysite (<2 μm) after: DS – DMSO intercalation; B – 1,3-butanediol grafting; HX – hexylamine intercalation; and T – deintercalation by toluene.

ite 001 peak, for MDS, M40DS, JDS, and HDS was 90%, 87%, 69%, and 30%, respectively. Differences in the degree of intercalation, obtained using the two methods, were caused by greater degrees of stacking order observed for the intercalated phase in comparison to the raw sample, which is noticeable for the H sample. Differences in the degree of intercalation may be related to the crystallinity of the starting material and also to the amount of structural stress accumulated (Deng *et al.*, 2002). The greatest degree of intercalation was recorded for well ordered 'Maria III' kaolinite, and it was less for poorly crystallized 'Jaroszów' kaolinite. Because the halloysite sample from the 'Dunino' deposit contains kaolinite, its degree of intercalation cannot be compared with those of other samples. Different degrees of intercalation in the reactions with formamide and DMSO, observed for the H sample, may be related to differences in dipole moment values of these compounds. The DMSO, with greater dipole moment (4.3 Debye), enters the interlayer space more easily than formamide with lesser dipole moment (3.7 Debye). Zhang and Xu (2007) suggested that the different intercalation behaviors of kaolin-group minerals can be attributed to the presence of amorphous SiO_2 particles

https://doi.org/10.1346/CCMN.2009.0570406 Published online by Cambridge University Press

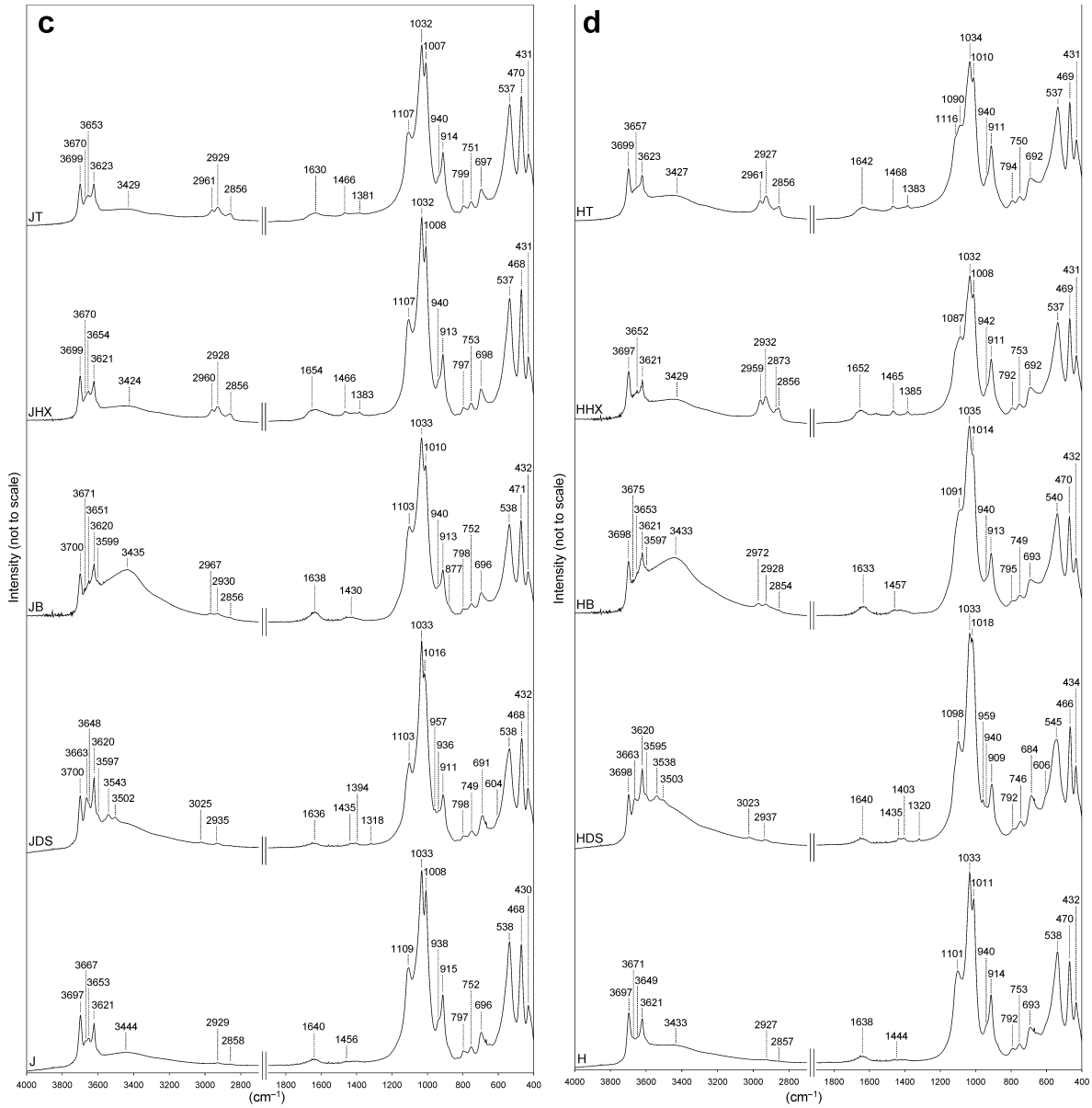

which block the access of DMSO molecules to the interlayer space of kaolin minerals; however, the existence of such particles was not recorded in the samples examined for the present study.

Interlayer grafting with 1,3 butanediol

As described by Gardolinski and Lagaly (2005b), the derivatives obtained in the procedure, where 1,3-butanediol was used for grafting reactions, showed predominantly tubes and rolled particles. Therefore, this diol was used for the experiments. The basal spacing, d_{001}, of 11.43 Å is characteristic of kaolinite with a 1,3-butanediol monolayer trapped in the interlayer space (Murakami *et al.*, 2004; Gardolinski and Lagaly, 2005a). In this arrangement, inner-surface OH groups of the mineral react with diol OH groups and Al-O-C covalent bonds are formed (Tunney and Detellier, 1993).

Although the experimental conditions were identical to those reported in the literature, only partially grafted minerals were synthesized (Figure 1). The reaction of MDS with 1,3-butanediol led to the formation of crystallites occupied by diol with different orientation with respect to kaolinite layers, as suggested by the presence of a broad reflection in the region from 7 to 12º2θ (MB). The reaction probably yielded an 8.6 Å hydrate of kaolinite (MB) (Costanzo *et al.*, 1984). The basal spacing of the unreacted kaolinite was also observed. The XRD pattern of the product formed in the reaction of the same mineral intercalate, but with particle size of <40 μm (M40DS), contained a similar

https://doi.org/10.1346/CCMN.2009.0570406 Published online by Cambridge University Press

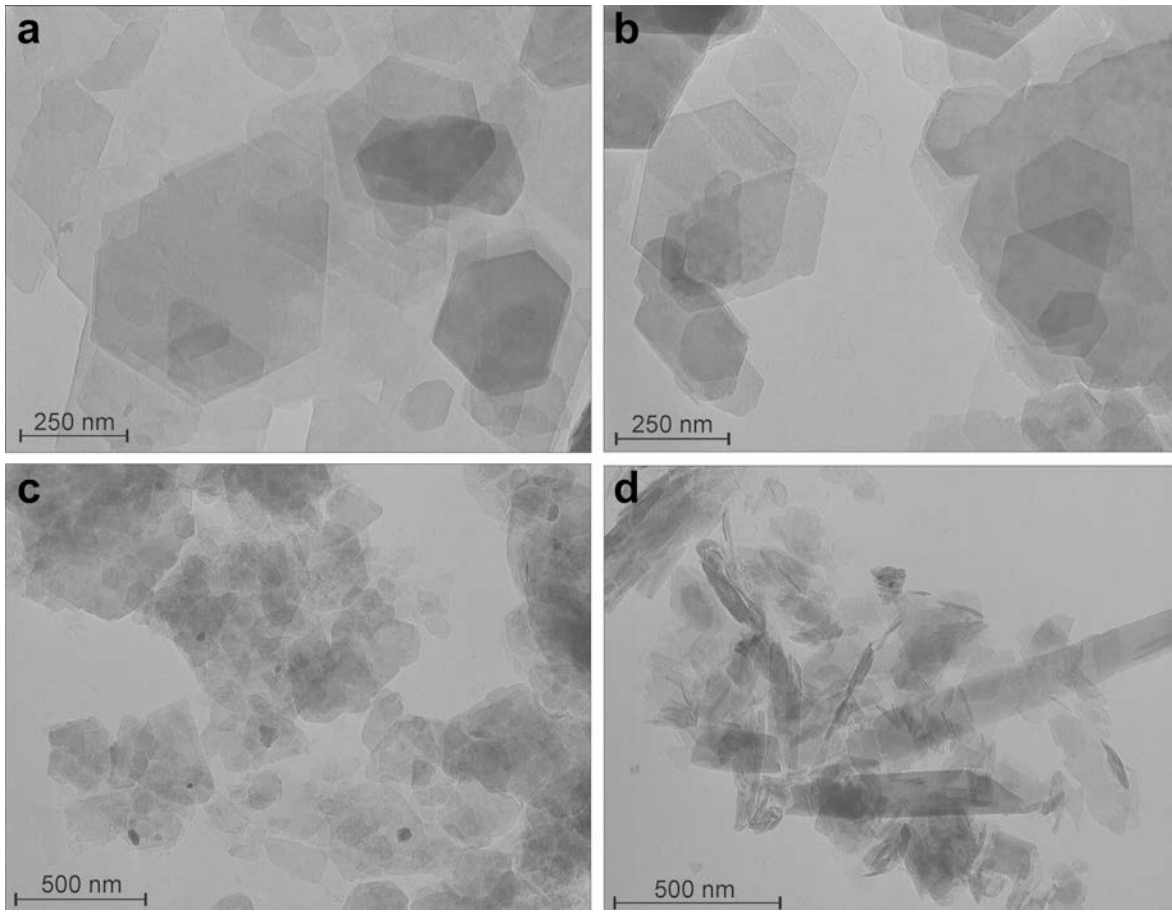

Figure 3. TEM images of raw samples: (a) M – 'Maria III' kaolinite (<2 μm); (b) M40 – 'Maria III' kaolinite (<40 μm); (c) J – 'Jaroszów' kaolinite (<2 μm); and (d) H – 'Dunino' halloysite (<2 μm).

broad reflection in the same region, but also had a well defined peak at 11.52 Å (M40B). This suggested a more uniform arrangement of diol molecules in the interlayer space of kaolinite. Reacting JDS with 1,3-butanediol produced a phase with a basal spacing of 10.63 Å (JB). In the reaction of HDS with diol, the formation of a grafted mineral with basal spacing of 11.09 Å (HB) was noticed.

The appearance of a broad band with a maximum at ~3433 cm^{-1} (diol OH stretching) and three bands at ~2900 cm^{-1} (C-H stretching) observed for the M40B, JB, and HB samples, confirmed that the diol molecules were trapped in the structures of these minerals (Figure 2). Even though a broad 3433 cm^{-1} band was less evident in the IR spectra of the MB sample, the appearance of a small band at 3599 cm^{-1} suggested that some diol molecules managed to form bonds with kaolinite (Figure 2a). The changes in relative intensities of the bands in the OH-stretching region (3700–3600 cm^{-1}) can also be attributed to the interaction of organic molecules with the crystal framework. The absence of the bands at ~3540 cm^{-1}, 3502 cm^{-1}, and 957 cm^{-1} confirmed that DMSO molecules were removed as the grafting process proceeded (Figure 2). Bands assigned to the in-plane Si-O-Si stretching vibrations and the perpendicular Si-O vibrations were shifted to positions characteristic of raw samples (Figure 2). The band assigned to Si-O-Si deformation was shifted to lower frequencies for the M40B, JB, and HB samples, while a shift to greater frequency was noticed for the MB sample. The changes in positions of the framework bands suggested that grafting contributed to a structural rearrangement of the samples. The Si/Al framework returned to a similar arrangement to that noticed for the raw samples.

Differential scanning calorimetry indicated that removal of diol molecules from the grafted compounds took place in the temperature range 200–400ºC (Figure 4). Calculations based on TG curves showed that the diol contents for the MB, M40B, JB, and HB samples were 1.92%, 2.74%, 2.34%, and 6.42%, respectively. The use of pre-intercalated minerals for

https://doi.org/10.1346/CCMN.2009.0570406 Published online by Cambridge University Press

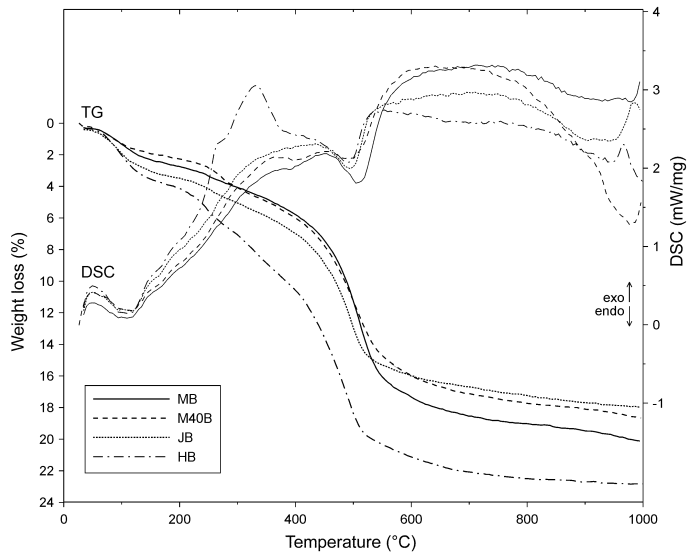

Figure 4. DSC-TG curves of kaolin-group minerals after grafting reaction with 1,3-butanediol: MB – 'Maria III' kaolinite (<2 μm), M40B – 'Maria III' kaolinite (<40 μm), JB – 'Jaroszów' kaolinite (<2 μm), HB – 'Dunino' halloysite (<2 μm).

grafting was essential. Apparently the grafting was a two-step process. Firstly, diol molecules entered the interlayer space and exchanged with DMSO, followed by the formation of Al-O-C covalent bonds. The intercalation and grafting of diol molecules could also have occurred simultaneously, to some extent. The results suggested that the reactivity of the selected kaolin minerals toward esterification with 1,3-butanediol increases with decreasing crystallinity of the starting material. Differences in the basal spacings between the results obtained in the present study and in previous studies may be caused by different positions of the diol molecules in the mineral structure and/or the presence of co-intercalated water. The rate of diffusion of DMSO and diol molecules, which is temperature dependent, as well as reaction time could influence grafting. Neither lowering the temperature of the process nor extending the reaction time to 48 h enhanced grafting efficiency (data not shown).

Hexylamine intercalation

The interlayer grafting was necessary in order to perform hexylamine intercalation. In the reactions of hexylamine with DMSO intercalates, without prior grafting, intercalation did not take place (data not shown). The degree of intercalation of amine was determined by the efficiency of the interlayer grafting. The XRD patterns (Figure 1) indicated that it was greatest for the poorly crystallized kaolinite 'Jaroszów' (JHX) and halloysite from the 'Dunino' deposit (HHX). The basal spacings of these derivatives were 22.1 Å and 25.6 Å, respectively. Higher-order reflections with maxima at 12.31 Å (HHX), 10.59 Å (JHX), and 8.20 Å (HHX) were also recorded. Basal-spacing values indicated the presence of amine chains which are nearly perpendicular to the basal-plane surfaces of minerals (Komori *et al.*, 1999; Gardolinski and Lagaly, 2005b). Komori *et al.* (1999) proved that alkyl chains take a bilayer arrangement, the amino groups react with inner-surface OH groups of the mineral from one side and with the tetrahedral sheet from the other side. Differences in spacing of ~3 Å may be related to the different arrangement of amine molecules in the mineral structure and/or the formation of kinks (Gardolinski and Lagaly, 2005b). Another possibility is the existence of a polyphase system consisting of particles containing layers with different amine arrangements and perhaps random interstratifications of such layers (Klapyta *et al.*, 2001). Although only partially grafted phases were formed in the reactions with 'Maria III' kaolinite (MB, M40B), the presence of small broad peaks at ~29.5 Å and 22.1 Å was recorded (MHX, M40HX). This indicated that some hexylamine molecules were intercalated. The XRD analyses suggested that the use of grafting products, in which diol molecules showed different orientations in the interlayer space, for amine intercalation reactions contributed to the formation of amine intercalates with low order in stacking of layers. For all of the intercalation reactions, a significant amount of unreacted kaolinite was observed.

Intercalation of amine gave rise to a band at ~1383 cm^{-1} (C-N stretching) and three bands in the C-H stretching region (3000–2800 cm^{-1}) which confirmed interaction of long organic chains with the mineral structures (Figure 2). Significant structural perturbations of the Si/Al framework, on the basis of lattice vibrations (1200–1000 cm^{-1}), were not observed (Figure 2).

https://doi.org/10.1346/CCMN.2009.0570406 Published online by Cambridge University Press

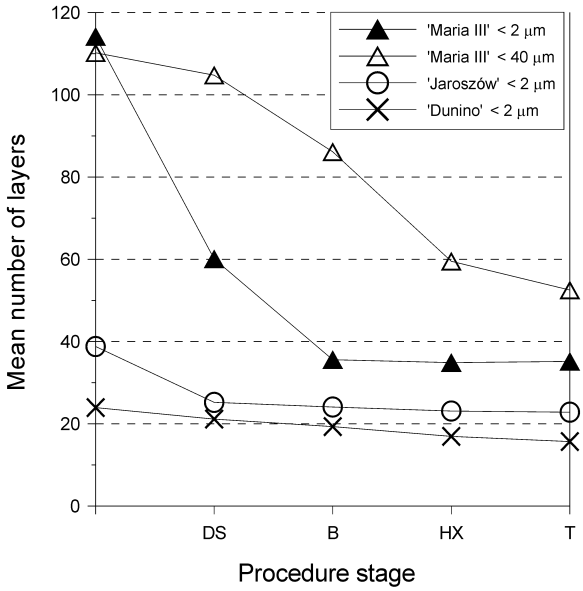

Figure 5. Changes in the average number of layers of kaolin-group minerals after: DS – DMSO intercalation; B– 1,3-butanediol grafting; HX – hexylamine intercalation; and T – deintercalation by toluene.

Deintercalation of hexylamine-intercalated minerals

The XRD patterns of deintercalated kaolin-group minerals (Figure 1) showed significant changes in comparison with those of amine-intercalated samples. For the 'Maria III' kaolinite, regardless of the particle size, peaks in the low-angle region disappeared (MT, M40T), indicating complete removal of amine. For the 'Jaroszów' kaolinite and the 'Dunino' halloysite, a decrease in intensity (JT, HT) and a position change (HT) for the amine intercalate 001 peak was observed. Moreover, the second-order reflections were shifted to 10.10 Å (JT) and 11.56 Å (HT) positions. Partial deintercalation was confirmed by a decrease in the intensity of the band at ~1383 cm^{-1} (C-N stretching) and the bands in the C-H stretching region (3000–2800 cm^{-1}) (Figure 2). The FTIR spectra in the region 1200–1000 cm^{-1} were not altered after deintercalation.

Delamination and structural changes in kaolin minerals

Changes in the mean number of layers in particles of kaolin-group minerals, after each experimental stage, were recorded (Figure 5). Raw 'Maria III' kaolinite particles (M, M40) consisted, on average, of ~110 layers, while raw 'Jaroszów' kaolinite (J) and 'Dunino' halloysite consisted of ~40 and ~25 layers, respectively. Accumulation of crystal defects, characteristic of the J and H samples, favored the formation of crystallites with fewer layers in contrast to low-defect M and M40 samples. Regardless of the initial mineral, a gradual decrease in the number of layers after each experimental step was observed. It was reduced considerably to ~35 and ~50 for the MT and M40T samples, and to 23 and 15 for the JT and HT samples, respectively. This confirmed that chemical treatment and subsequent modifications of the interlayer environment led to extensive delamination of the particles.

Such functionalization processes strongly affected the structural arrangement of the treated minerals. Earlier studies based on detailed analysis of diffraction profiles revealed that the major defect in kaolinites is the

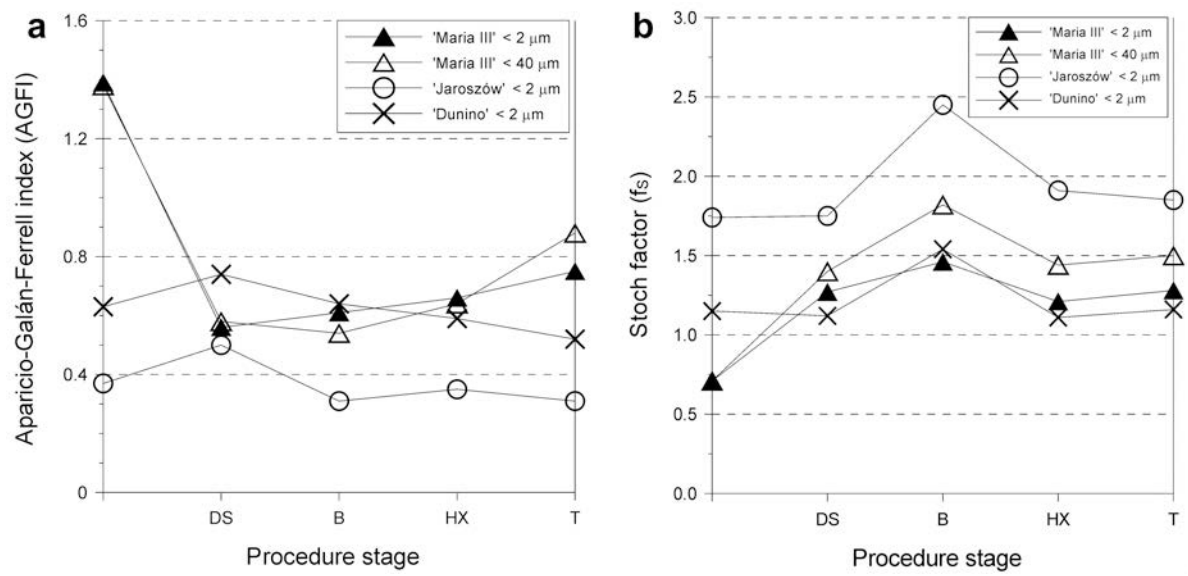

Figure 6. Changes in the Aparicio-Galán-Ferrell index (AGFI) (a) and Stoch factor (f_S) (b) for kaolin-group minerals after: DS – DMSO intercalation, B – 1,3-butanediol grafting; HX – hexylamine intercalation, and T – deintercalation by toluene.

https://doi.org/10.1346/CCMN.2009.0570406 Published online by Cambridge University Press

existence of interlayer shifts (t_1, t_2) between neighboring layers: t_1 (~$-a/3$) and t_2 (~$-a/3 + b/3$); another possibility is the occurrence of layers with vacant *C* sites (Plançon *et al.*, 1989; Plancon and Zacharie, 1990). Kogure and Inoue (2005) observed the interlayer displacements of kaolinite layers using high-resolution transmission electron microscopy (HRTEM) confirming the earlier studies. Crystallinity indexes do not provide information concerning the types of structural defects (Plançon *et al.*, 1988). Therefore, AGFI and f_S were only used in order to assign a numerical value to the degree of structural disorder and to evaluate the abundance of translation defects (Figure 6). All kaolin minerals were subjected to modifications by organic compounds leading to qualitative structural changes. Note that investigations based on the AGFI and f_S values obtained may only be used to determine a general trend showing the relation between structural order and chemical treatment. The XRD profile in the 20–23°2θ region, used to calculate the indexes, contains information about the modified mineral as well as the untreated mineral. Both AGFI and f_S indicated that, regardless of the particle size, the first two experimental stages (DS, B) led to a considerable decrease in the structural order for 'Maria III' kaolinite (Figure 6). The f_S values suggested that grafting reactions contributed to the greatest increase in structural disorder in kaolin minerals (Figure 6b). The changes in the structural order indexes were most evident for the 'Maria III' kaolinites and were less noticeable for the 'Jaroszów' kaolinite and for the 'Dunino' halloysite.

TEM analyses

Observations of the morphology were performed using TEM in order to examine the rolling of the kaolinite layers. Deintercalation of the amine-intercalated minerals led to a reduction of the structural rigidity and weakening of the interlayer hydrogen bonds. As a result, individual layers of particles formed hollow tubes. In nature, transformation of kaolinite to halloysite may be initiated by hydration of layers, leading to a decrease in the structural rigidity of the crystals and subsequent curling (Robertson and Eggleton, 1991). Rolled particles were present in all samples, though the amount present was related to the efficiency of the intercalation/deintercalation stages. For the 'Jaroszów' kaolinite (Figure 7) and 'Dunino' halloysite (Figure 8), where intercalation and grafting processes were more intense, the occurrence of particles exhibiting tubular morphology was more frequent than in samples of 'Maria III' kaolinite (Figure 9), where chemical modifications were less effective. The mean diameter of nanotubes, regardless of the starting material, was ~30 nm which indicated bending of individual delaminated layers (Bates *et al.*, 1950; Gardolinski and Lagaly, 2005b). Their length clearly depended on the particle size of the starting minerals and varied from 150 to 500 nm. Some particles were only partially rolled, thus showing the process of layer curling (Figure 7c). Figure 9b shows a particle where bending was accomplished only from one side. Layers of larger crystallites tend to roll more than once until a fully developed tube is formed as can be concluded from the unrolled upper ending of the particle (Figure 9b). The particle shown in

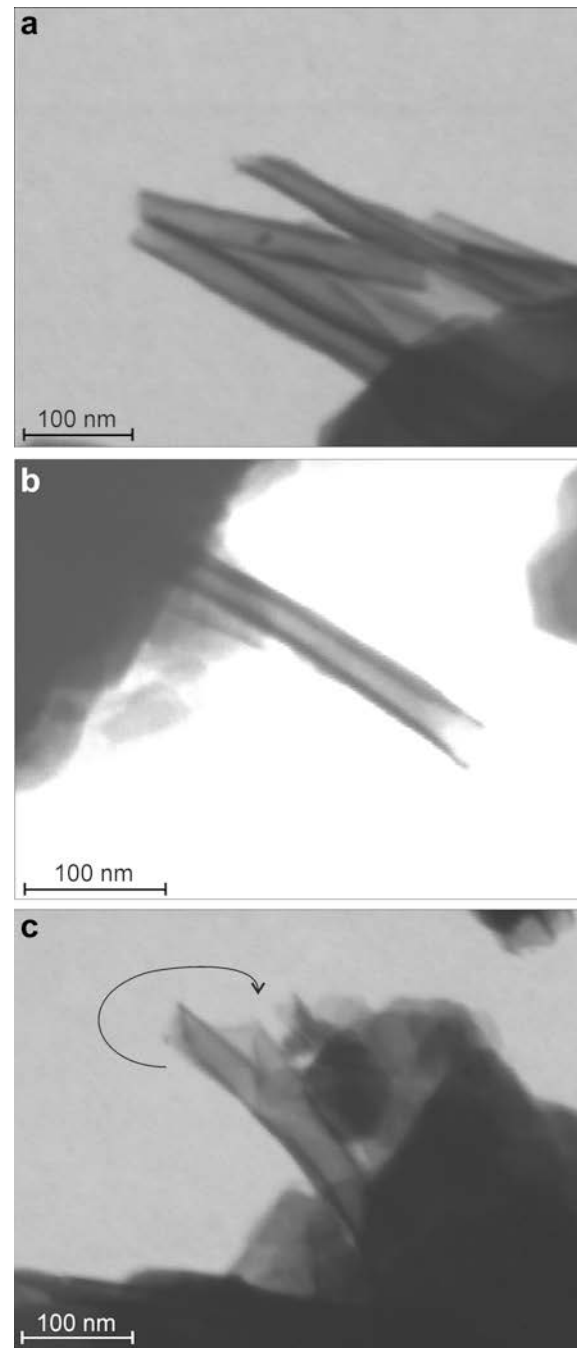

Figure 7. TEM images of 'Jaroszów' kaolinite after the intercalation/deintercalation process.

https://doi.org/10.1346/CCMN.2009.0570406 Published online by Cambridge University Press

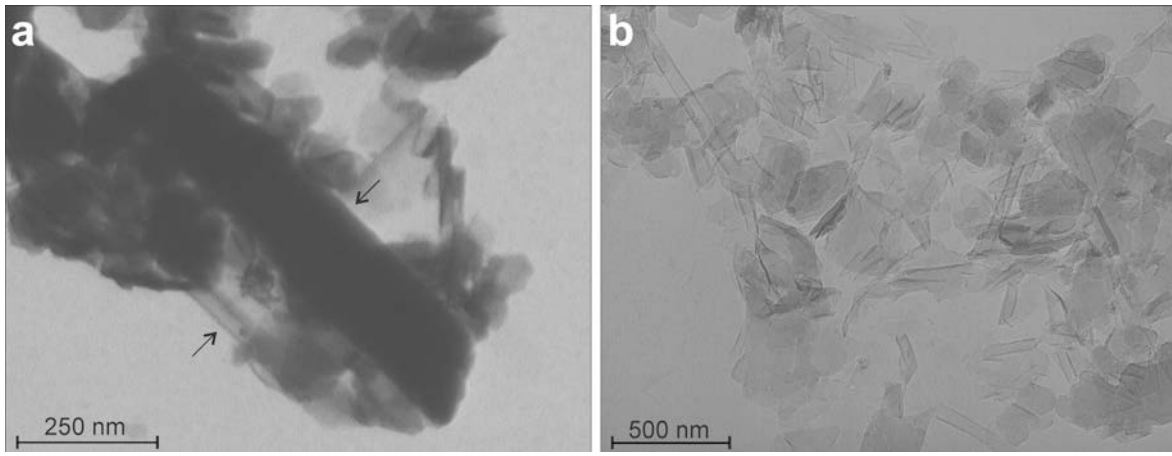

Figure 8. TEM images of 'Dunino' halloysite after the intercalation/deintercalation process.

Figure 9c suggests that the formation of tubes was initiated by delamination of surface layers. This was followed by rolling of partially detached layers along crystal faces (marked by arrows). As a result, curved plates were still connected to the kaolinite particles, suggesting that repeated intercalation/deintercalation should enhance the number of rolled plates by affecting layers which are located deeper within the particles. Apart from the nanotubes formed due to the intercalation/deintercalation procedure, the 'Dunino' halloysite sample also consisted of naturally occurring halloysite tubes (Figure 8a). These tubular particles were much larger than those obtained experimentally, with diameters of ~100 nm and >500 nm long. The presence of both types of tubes indicated that the applied experimental procedure produced new nanotubes while the morphology of natural tubes was unaffected. Planar particles of raw kaolinite were still present after reactions in all cases.

CONCLUSIONS

The ability to roll kaolinite layers by means of intercalation/deintercalation was demonstrated. The increase in basal spacing induced by the presence of long-chain amine reduces the strength of the hydrogen bonds and subsequently favors separation and curling of the layers. In the more ordered kaolinites, chemical treatment caused a remarkable increase in structural disorder and led to extensive delamination of crystallites. Kaolinite particles which exhibited tubular morphology or showed rolling effects were observed using TEM. The nanotubes formed had mean diameters of ~30 nm and their lengths (150−500 nm) were related to the particle size of the initial mineral. The number of rolled kaolinite layers depended heavily on the efficiency of the intercalation steps. More nanotubes were observed for the more disordered 'Jaroszów' kaolinite and for the 'Dunino' halloysite, where the intercalation processes were more efficient than in the reactions with

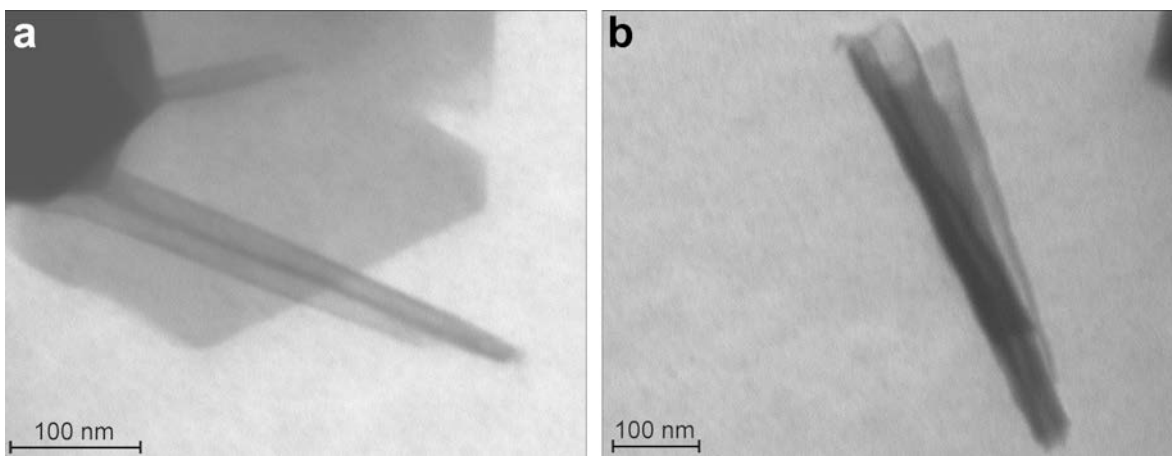

Figure 9. TEM images of 'Maria III' kaolinite after the intercalation/deintercalation process.

https://doi.org/10.1346/CCMN.2009.0570406 Published online by Cambridge University Press

the more ordered 'Maria III' kaolinite. Natural halloysite nanotubes which were observed in the 'Dunino' sample were not affected by the experimental procedure applied.

ACKNOWLEDGMENTS

The authors are indebted to Dr J. Sołtys, Managing Director of the 'Intermark' company, for supplying the mineral samples from the 'Dunino' deposit. They are grateful to Dr G.J. Churchman (University of Adelaide) and two anonymous referees for critical reading and constructive reviews. They are also grateful to Professor E.M. Serwicka for helpful discussion. This work was supported financially by the Ministry of Science and Higher Education under research project No. N N307 315336 (2009-2012).

REFERENCES

Aparicio, P., Galán, E., and Ferrell, R.E. (2006) A new kaolinite order index based on XRD profile fitting. *Clay Minerals*, **41**, 811–817.

Bahranowski, K., Serwicka, E.M., Stoch, L., and Strycharski, P. (1993) On the possibility of removal of non-structural iron from kaolinite-group minerals. *Clay Minerals*, **28**, 379–391.

Bates, T.F., Hildebrand, F.A., and Swineford, A. (1950) Morphology and structure of endellite and halloysite. *American Mineralogist*, **35**, 463–484.

Brigatti, M.F., Galán, E., Theng, B.K.G., and Lagaly, G. (2006) Structures and mineralogy of clay minerals. Pp. 19–87 in: *Handbook of Clay Science*. *Developments in Clay Science, Vol. 1* (F. Bergaya, B.K.G. Theng and G. Lagaly, editors). Elsevier, Amsterdam.

Churchman, G.J., Whitton, J.S., Claridge, G.G.C., and Theng, B.K.G. (1984) Intercalation method using formamide for differentiating halloysite from kaolinite. *Clays and Clay Minerals*, **32**, 241–248.

Costanzo, P.M., Giese Jr, R.F., and Lipsicas, M. (1984) Static and dynamic structure of water in hydrated kaolinites. I. The static structure. *Clays and Clay Minerals*, **32**, 419–428.

Deng, Y., White, G.N., and Dixon, J.B. (2002) Effect of structural stress on the intercalation rate of kaolinite. *Journal of Colloid and Interface Science*, **250**, 379–393.

Dong, W., Li, W., Yu, K., Krishna, K., Song, L., Wang, X., Wang, Z., Coppens, M.O., and Feng, S. (2003) Synthesis of silica nanotubes from kaolin clay. *Chemical Communications*, **11**, 1302–1303.

Elbokl, T.A. and Detellier, C. (2006) Aluminosilicate nanohybrid materials. Intercalation of polystyrene in kaolinite. *Journal of Physics and Chemistry of Solids*, **67**, 950–955.

Farmer, V.C. (1974) The layer silicates. Pp. 331–363 in: *The Infrared Spectra of Minerals* (V.C. Farmer, editor). Mineralogical Society, London.

Farmer, V.C. and Russell, J.D. (1967) Infrared absorption spectrometry in clay studies. *Clays and Clay Minerals*, **15**, 121–142.

Gardolinski, J.E.F.C. and Lagaly, G. (2005a) Grafted organic derivatives of kaolinite: I. Synthesis, chemical and rheological characterization. *Clay Minerals*, **40**, 537–546.

Gardolinski, J.E.F.C. and Lagaly, G. (2005b) Grafted organic derivatives of kaolinite: II. Intercalation of primary n-alkylamines and delamination. *Clay Minerals*, **40**, 547–556.

Hayashi, S. (1997) NMR study of dynamics and evolution of guest molecules in kaolinite/dimethylsulfoxide intercalation compound. *Clays and Clay Minerals*, **45**, 724–732.

Hinckley, D.N. (1962) Variability in 'Crystallinity' values among the kaolin deposits of the coastal plain of Georgia and South Carolina. *Clays and Clay Minerals*, **11**, 229–235.

Hope, E.W. and Kittrick, J.A. (1964) Surface tension and the morphology of halloysite. *American Mineralogist*, **49**, 859–866.

Inagaki, S., Fukushima, Y., and Kuroda, K. (1993) Synthesis of highly ordered mesoporous materials from a layered polysilicate. *Journal of the Chemical Society, Chemical Communications*, **8**, 680.

Joussein, E., Petit, S., Churchman, J., Theng, B., Righi, D., and Delvaux, B. (2005) Halloysite clay minerals – a review. *Clay Minerals*, **40**, 383–426.

Klapyta, Z., Fujita, T., and Iyi, N. (2001) Adsorption of dodecyl- and octadecyltrimethylammonium ions on a smectite and synthetic micas. *Applied Clay Science*, **19**, 5–10.

Kogure, T. and Inoue, A. (2005) Determination of defect structures in kaolin minerals by high-resolution transmission electron microscopy (HRTEM). *American Mineralogist*, **90**, 85–89.

Komori, Y., Sugahara, Y., and Kuroda, K. (1999) Intercalation of alkylamines and water into kaolinite with methanol kaolinite as intermediate. *Applied Clay Science*, **15**, 241–252.

Lin, H.P. and Mou, C.Y. (1996) 'Tubules-Within-a-Tubule' Hierarchical Order of Mesoporous Molecular Sieves in MCM-41. *Science*, **273**, 765.

Liu, M., Guo, B., Du, M., Lei, Y., and Jia, D. (2008) Natural inorganic nanotubes reinforced epoxy resin nanocomposites. *Journal of Polymer Research*, **15**, 205–212.

Machado, G.S., Freitas Castro, K.A.D., Wypych, F., and Nakagaki, S. (2008) Immobilization of metalloporphyrins into nanotubes of natural halloysite toward selective catalysts for oxidation reactions. *Journal of Molecular Catalysis A: Chemical*, **283**, 99–107.

Madhusoodana, C.D., Kameshima, Y., Nakajima, A., Okada, K., Kogure, T., and MacKenzie, K.J.D. (2006) Synthesis of high surface Al-containing mesoporous silica from calcined and acid leached kaolinites as the precursors. *Journal of Colloid and Interface Science*, **297**, 724–731.

Murakami, J., Itagaki, T., and Kuroda, K. (2004) Synthesis of kaolinite-organic nanohybrids with butanediols. *Solid State Ionics*, **172**, 279–282.

Murray, H.H. (2000) Traditional and new applications for kaolin, smectite and palygorskite: a general overview. *Applied Clay Science*, **17**, 207–221.

Nakagaki, S. and Wypych, F. (2007) Nanofibrous and nanotubular supports for the immobilization of metalloporphyrins as oxidation catalysts. *Journal of Colloid and Interface Science*, **315**, 142–157.

Nakagaki, S., Machado, G.S., Halma, M., Santos Marangon, A.A., Freitas Castro, K.A.D., Mattoso, N., and Wypych, F. (2006) Immobilization of iron porphyrins in tubular kaolinite obtained by an intercalation/delamination procedure. *Journal of Catalysis*, **242**, 110–117.

Olejnik, J., Aylmore, L.A.G., Posner, A.M., and Quirk, J.P. (1968) Infrared spectra of kaolin mineral-dimethyl sulfoxide complexes. *Journal of Physical Chemistry*, **72**, 241–249.

Patterson, A.L. (1939) The Scherrer formula for X-ray particle size determination. *Physical Review*, **56**, 978–982.

Plançon, A. and Zacharie, C. (1990) An expert system for the structural characterization of kaolinites. *Clay Minerals*, **25**, 249–260.

Plançon, A., Giese, R.F., and Snyder, R. (1988) The Hinckley index for kaolinites. *Clay Minerals*, **23**, 249–260.

Plançon, A., Giese, R.F., Snyder, R., Drits, V.A., and Bookin, A.S. (1989) Stacking faults in the kaolin-group-minerals: Defect structures of kaolinite. *Clays and Clay Minerals*, **37**, 203–210.

Poyato-Ferrera, J., Becker, H.O., and Weiss, A. (1977) Phase

changes in kaolinite-amine-complexes. *Proceedings of the International Clay Conference, Oslo*, 148–150.

Robertson, I.D.M. and Eggleton, R.A. (1991) Weathering of granitic muscovite to kaolinite and halloysite and of plagioclase-derived kaolinite to halloysite. *Clays and Clay Minerals*, **39**, 113–126.

Serwicka, E.M. and Bahranowski, K. (2004) Environmental catalysis by tailored materials derived from layered minerals. *Catalysis Today*, **90**, 85–92.

Singh, B. (1996) Why does halloysite roll? – A new model. *Clays and Clay Minerals*, **44**, 191–196.

Singh, B. and Mackinnon, I.D.R. (1996) Experimental transformation of kaolinite to halloysite. *Clays and Clay Minerals*, **44**, 825–834.

Stoch, L. (1974) *Mineraly Ilaste ('Clay Minerals')*. Geological Publishers, Warsaw.

Thompson, J.G. and Cuff, C. (1985) Crystal structure of kaolinite: dimethylsulfoxide intercalate. *Clays and Clay Minerals*, **33**, 490–500.

Tunney, J.J. and Detellier, C. (1993) Interlamellar covalent grafting of organic units on kaolinite. *Chemistry of Materials*, **5**, 747–748.

Tunney, J.J. and Detellier, C. (1997) Interlamellar amino functionalization of kaolinite. *Canadian Journal of Chemistry*, **75**, 1766–1772.

Weiss, A. and Russow, J. (1963) Uber das Einrollen von Kaolinitkristallen zu halloysitahnlichen rohren und einen unterschied zwischen halloysit und rohrchenformigem kaolinit. *Proceedings of the International Clay Conference, Stockholm*, **2**, 69–79.

Wiewióra, A. and Brindley, G.W. (1969) Potassium acetate intercalation in kaolinite and its removal: Effect of material characteristics. *Proceedings of the International Clay Conference, Tokyo*, **1**, 723–733.

Zhang, X. and Xu, Z. (2007) The effect of microwave on preparation of kaolinite/dimethylsulfoxide composite during intercalation process. *Materials Letters*, **61**, 1478–1482.

Zimowska, M., Michalik-Zym, A., Połtowicz, J., Bazarnik, M., Bahranowski, K., and Serwicka, E.M. (2007) Catalytic oxidation of cyclohexane over metalloporphyrin supported on mesoporous molecular sieves of FSM-16 type – steric effects induced by nanospace constraints. *Catalysis Today*, **124**, 55–60.

(*Received 25 November 2008; revised 20 June 2009; Ms. 0236; A.E. D.C. Bain*)